AD-A153 608 PROJECTIONS OF PLASMA CLOUD STRUCTURES AND THEIR SPECTRA(U) NAVAL RESEARCH LAB WASHINGTON DC N J ZABUSKY ET AL. 22 APR 85 NRL-MR-5561 1/1

UNCLASSIFIED F/G 20/9 NL

END

FILMED

DTIC

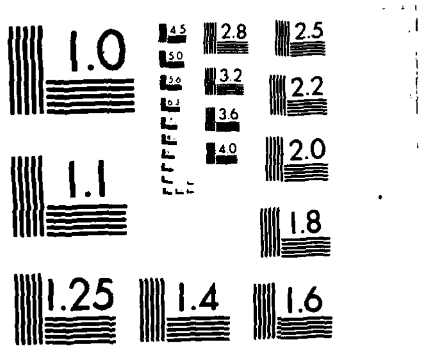
1.0
1.1
1.25
1.4
1.6
1.8
2.0
2.2
2.5
2.8
3.2
3.6
4.0

NRL Memorandum Report 5561

Projections of Plasma Cloud Structures and their Spectra

N. J. ZABUSKY

Fluid Sciences, Inc.
Pittsburgh, PA 15217

E. HYMAN

Science Applications International Corporation
McLean, VA 22102

M. MULBRANDON

Geophysical and Plasma Dynamics Branch
Plasma Physics Division

April 22, 1985

This research was sponsored by the Defense Nuclear Agency under Subtask S99QMXRI, work unit 00018 and work unit title "Infrared Structure."

NAVAL RESEARCH LABORATORY
Washington, D.C.

85

SECURITY CLASSIFICATION OF THIS PAGE

REPORT DOCUMENTATION PAGE

1a REPORT SECURITY CLASSIFICATION: UNCLASSIFIED

1b RESTRICTIVE MARKINGS:

2a SECURITY CLASSIFICATION AUTHORITY:

2b DECLASSIFICATION / DOWNGRADING SCHEDULE:

3 DISTRIBUTION / AVAILABILITY OF REPORT: Approved for public release; distribution unlimited.

4 PERFORMING ORGANIZATION REPORT NUMBER(S): NRL Memorandum Report 5561

5 MONITORING ORGANIZATION REPORT NUMBER(S):

6a NAME OF PERFORMING ORGANIZATION: Naval Research Laboratory

6b OFFICE SYMBOL (If applicable): Code 4780

7a NAME OF MONITORING ORGANIZATION:

6c ADDRESS (City, State, and ZIP Code): Washington, DC 20375-5000

7b ADDRESS (City, State, and ZIP Code):

8a NAME OF FUNDING / SPONSORING ORGANIZATION: Defense Nuclear Agency

8b OFFICE SYMBOL (If applicable): RAAE

9 PROCUREMENT INSTRUMENT IDENTIFICATION NUMBER:

8c ADDRESS (City, State, and ZIP Code): Washington, DC 20305

10 SOURCE OF FUNDING NUMBERS

PROGRAM ELEMENT NO.	PROJECT NO	TASK NO.	WORK UNIT ACCESSION NO.
62715H			DN080-323

11 TITLE (Include Security Classification): Projections of Plasma Cloud Structures and their Spectra

12 PERSONAL AUTHOR(S): Zabusky, N.J.,* Hyman, E.,† and Mulbrandon, M.

13a. TYPE OF REPORT	13b. TIME COVERED	14. DATE OF REPORT (Year, Month, Day)	15. PAGE COUNT
Interim	FROM 10/83 TO 10/84	1985 April 22	31

16 SUPPLEMENTARY NOTATION *Fluid Sciences, Inc., Pittsburgh, PA 15217
†Science Applications International Corporation, McLean, VA 22102 (Continues)

17 COSATI CODES

FIELD	GROUP	SUB-GROUP

18. SUBJECT TERMS (Continue on reverse if necessary and identify by block number): Spectral index, Power spectral density, Plasma cloud scan, Cloud contour. (Continues)

19 ABSTRACT (Continue on reverse if necessary and identify by block number)

We have established a relationship between the asymptotic spectral index of idealized piecewise-constant (pc) optically-thin radiating sources and their scans. For piecewise-constant clouds, where the one-dimensional asymptotic spectrum of the power is proportional to k^{-2}, we have shown that the asymptotic spectrum of the scan depends upon the character of the contour, at the point $\underset{\sim}{x}_0 \equiv (x_0, y_0)$ where it is tangent to the extremal ray. If the contour at $(\underset{\sim}{x}_0)$ behaves like $y-y_0 = \gamma (x-x_0)^\tau$ then the (Continues)

20 DISTRIBUTION / AVAILABILITY OF ABSTRACT: ☒ UNCLASSIFIED/UNLIMITED ☐ SAME AS RPT ☐ DTIC USERS

21 ABSTRACT SECURITY CLASSIFICATION: UNCLASSIFIED

22a NAME OF RESPONSIBLE INDIVIDUAL: J. D. Huba

22b TELEPHONE (Include Area Code): (202) 767-3630

22c OFFICE SYMBOL: Code 4780

DD FORM 1473, 84 MAR — 83 APR edition may be used until exhausted. All other editions are obsolete

SECURITY CLASSIFICATION OF THIS PAGE

16. SUPPLEMENTARY NOTATION (Continued)

This research was sponsored by the Defense Nuclear Agency under Subtask S99QMXRI, work unit 00018 and work unit title "Infrared Structure."

18. SUBJECT TERMS (Continued)

Spatial structuring
PLACES experiment

19. ABSTRACT (Continued)

asymptotic spectral envelope of the PSD of the scan varies as $k^{-2(\tau + 1)}$. For a convex curve with finite curvature at $\underset{\sim}{x}_0$, we have $\tau = 1/2$ and obtain the well-known result, k^{-3}. In addition, if the radiating density in such a cloud flank varies with a power law m, then the asymptotic spectral envelope of the scan's PSD varies as $k^{-2(1 + \tau + m)}$. We also apply the results to the interpretation of optical scans from two PLACES events. These are insufficiently resolved and their estimated spectral index of 2.5 is associated with a composite of effects and not the nonlinear dynamics of striation evolution.

CONTENTS

PROJECTIONS OF PLASMA CLOUD STRUCTURES AND THEIR SPECTRA

1. INTRODUCTION

Observation of unstable and turbulent geophysical fluid dynamical processes are often indirect and made from remote sensors. Many processes are observed optically from several vantage points and the spatial radiance distribution is recorded photographically or electronically. From successive frames, one hopes to deduce the location and morphology of evolving hierarchies of structures. Unfortunately, a detailed reconstruction is impossible because of the lack of precise control of the processes that govern the radiation, the paucity of recording locations, and the lack of detailed in-situ (rocket borne) diagnostics. That is, compared to the progress in laboratory tomography, our problem is highly underdetermined.[1,2]

A long-range goal of the present investigation is to construct simple models of radiating ionospheric or HANE plasma clouds that are useful to communication and tracking systems engineers. We are interested in the: intercloud distances, scale sizes, gradients and asymmetries with respect to the earth's magnetic field and ambient winds and the evolution of these structural features. We will distill the bits of information available from field experiments and large-scale nonlinear dynamical computer simulations into cogent models. Conventionally, one discretizes field data and uses the computed power spectral densities (PSD's) to compare with realistic turbulent or wave steepening numerical simulations. However, PSD's and their spectral exponents are subject to errors because of the inadequacy of resolution and dynamical range in experimental and numerical simulation data. Some considerations of the latter were given in the first report of this series[3] and are applied here.

In Section 2 we discuss the relation between radiation from an idealized (piecewise-constant, pc) cloud and its projection functions, f(x). These are intensity scans through a "slice" of the cloud. For simplicity, the cloud is taken to be sufficiently remote so that parallax

Manuscript approved January 28, 1985.

effects are negligible. That is, all rays emitted by the cloud are perpendicular to the projection plane. We will show that essential properties of f(x) are related to properties of the cloud's boundary curve (e.g., curvature, etc.) at points where projection rays are tangent to the boundary curve. We also examine the competition between local curvature and density gradient at a tangent ray to clouds. In Section 3 we relate PSD's of clouds to the PSD's of their projection functions. In Section 4 we analyze measured scans from two "PLACES" experiments in light of the above results, and Section 5 presents our conclusions.

2. PROJECTIONS OF 3D CLOUDS

2.1 Introduction

Ionospheric plasma cloud densities may be approximated by the separable function

$$n(\underset{\sim}{x}', t) = n_{\perp}(x', y', t) g_{\parallel}(z', t) \qquad (1)$$

where z' is along the earth's magnetic field. Thus $n_{\perp}$ exhibits a steep "backside" and $g_{\parallel}$ may be approximated by $\exp - [(z' - z_0)/\ell]^2$ where $\ell^2 = \ell_0^2 + (\nu t)$ approximates a diffusive spreading along z' with diffusivity ν and $z_0(t)$ decreases in time as the cloud settles from its high altitude release point. There is evidence that the symmetry in $z' - z_0$ may be broken in time, that is, the higher altitude regions may be more diffuse.[4] However, to illustrate the nature of projections and the essential issues involved in computing PSD's we suppress the time variable and consider an idealized cloud with piecewise constant (pc) density in a bounded domain D, namely

$$n = \begin{cases} F_0 & \underset{\sim}{x} \in D \\ 0 & \underset{\sim}{x} \notin D \end{cases} \qquad (2)$$

2.2 Piecewise-Constant Clouds.

Figure 1 shows a segment of a pc cloud, the curve $C(x,y) = 0$ (which is the intersection of domain D and $P(\underset{\sim}{x})$, the perpendicular intersection plane) and the projection plane on which the radiance image is recorded. The sketch to the right of the plane is an intensity plot f(x) associated with a "slice", the line a-b on the projection plane. For an optically thin cloud, $f(x)$ is obtained by integrating the intersection intensity, $f_I(x,y)$, along the y direction (perpendicular to the projection plane). The limits of integration $y_+(x)$ and $y_-(x)$ are the intersections of a line perpendicular to the projection plane with $C(x,y) = 0$. That is

$$f(x) = \int_{-y_-(x)}^{+y_+(x)} dy\, f_I(x,y) = F_0\{y_+(x) + y_-(x)\} \equiv F_0 y(x). \tag{3}$$

Generally, for non-pc clouds $f_I(x,y)$ will not be constant and will depend on the orientation angle of the viewer with respect to the magnetic field and ambient wind.

Consider $f(x)$ near $x = x_0$ where a projection ray is tangent on the left to $C(x,y) = 0$, (e.g., point a in Fig. 1). Thus, for $x > x_0$ we represent the curve <u>locally</u> for $y > y_0$ by

$$x - x_0 = t, \tag{4a}$$

$$y - y_0 = \gamma t^{\tau}, \tag{4b}$$

where $t \to (0+)$. That is, the right side of (4a) and (4b) may be considered the leading terms in a series in t, which represent an arbitrary curve. Thus,

$$y_x \equiv y_t/x_t = \tau\gamma t^{\tau-1}, \tag{5}$$

is singular, constant, or zero as $t \to 0$ if $\tau < 1.0$, $\tau = 1.0$ or $\tau > 1.0$, respectively. Similarly, the curvature

$$\kappa \equiv \frac{y_{tt}x_t - x_{tt}y_t}{\{x_t^2 + y_t^2\}^{3/2}} = \frac{\gamma\tau(\tau-1)t^{(-2\tau+1)}}{\{t^{2-2\tau} + \tau^2\gamma^2\}^{3/2}}, \quad (\tau < 1) \tag{6}$$

is singular, constant or zero as $t \to 0$ if $\tau > 1/2$, $\tau = 1/2$, or $\tau < 1/2$, respectively. The table below summarizes some cases in the vicinity of $\underset{\sim}{x} = \underset{\sim}{x}_0$.

Table 1. Various Curves, (Equation 4) Near an Extremal Ray and The Asymptotic Behavior of the PSD for Piecewise-Constant Regions

τ	LOCAL FUNCTIONAL FORM	$y_x(\underset{\sim}{x}_0)$	$\kappa(\underset{\sim}{x}_0)$	FIG. 2	ASYMPTOTIC BEHAVIOR OF PSD FOR PC REGIONS
2.0	$y-y_0 = \pm\gamma(x-x_0)^2$	0	∞	(NOT SHOWN)	k^{-6}
4/3	$y-y_0 = \pm\gamma(x-x_0)^{4/3}$	0	∞	CUSP (NOT SHOWN)	$k^{-14/3}$
1.0	$y-y_0 = \pm\gamma(x-x_0)$	γ	∞	CORNER (NOT SHOWN)	k^{-4}
2/3	$y-y_0 = \pm\gamma(x-x_0)^{2/3}$	∞	∞	(NOT SHOWN)	$k^{-10/3}$
1/2	$y-y_0 = \pm\gamma(x-x_0)^{1/2}$	∞	$-2/\gamma^2$	●	k^{-3}
1/3*	$y-y_0 = \gamma(x-x_0)^{1/3}$	∞	0	Δ	$k^{-8/3}$
1/4	$y-y_0 = \pm\gamma(x-x_0)^{1/4}$	∞	0	□	$k^{-5/2}$
$\varepsilon<<1$	$y-y_0 = \pm\gamma(x-x_0)^{\varepsilon}$	∞	0	(NOT SHOWN)	$k^{-(2+2\varepsilon)}$

*All cases are for $x > x_0$ except $\tau = 1/3$ which applies for $-\infty < x < \infty$

The next to last column refers to illustrations given in Figure 2. The last column gives the asymptotic behavior of the PSD for pc densities (i.e $m = 0$, as discussed in Sec 3.2).

For example, the elliptical limacon

$$\{x,y\} = \{1-\mu \cos \theta\}\{\alpha \cos \theta, \beta \sin \theta\}, \tag{7}$$

has a curvature

$$\kappa = \alpha\beta\{1 + 2\mu^2 - 3\mu \cos \theta\}/D^{3/2}, \tag{8}$$

where

$$D = \alpha^2\{\sin\theta - \mu\sin 2\theta\}^2 + \beta^2\{\cos\theta - \cos 2\theta\}^2. \tag{9}$$

From (8) one obtains $\kappa = 0$ at $\theta = 0$ if $\mu = 1/2$ and

$$\{y/\beta\} = \{2\}^{-1/4}\,\{\frac{\alpha}{2} - x\}^{1/4} + \ldots\quad, \tag{10}$$

which corresponds to the $\tau = 1/4$ entry in Table 1. More realistic clouds may be composed by summing many nested pc clouds and each one will contribute its own projection function.

2.3 Finite-gradient Clouds.

We now consider more realistic $n(\underset{\sim}{x})$ with finite gradients near the edge of the boundary of the domain. Hence $f_I(x,y)$ is no longer constant within the contour of intersection $C(x,y)$ and we have two competing space scales at the tangency points, namely, the local radius of curvature and the local gradient scale, $\ell = f_I/|\nabla f_I|$.

To elucidate this competition, we perform a local analysis for a structure with a polynomial flank of degree m

$$f_I = x_0^{-m}\,[(x_b - x)^2 + (y_b - y)^2]^{m/2}\,F_0, \qquad x_0 - |\varepsilon| < x < x_0\ , \tag{11}$$

where (x_b, y_b) are on the boundary such that

$$\frac{y}{x} = \frac{(y_b - y)}{(x_b - x)},$$

or

$$x_b = x_0 - \{\frac{x_b y}{x\,\gamma}\}^{\frac{1}{\tau}}. \tag{12}$$

To lowest order this is

$$x_b = x_0 - \{\frac{x_0 y}{x\,\gamma}\}^{\frac{1}{\tau}}.$$

At fixed x, one evaluates

$$f = 2\int_0^{y_+} f_I(x,y)\,dy,$$

where $y_+ = \gamma(x_0 - x)^\tau$. Near $x = x_0$, one expands the terms in parenthesis and retains only the lowest order in y, $O(y^2)$, and after some algebra obtains

$$f \approx 2x_0^{-m} F_0 \gamma(x_0 - x)^{m+\tau} + O(x_0 - x)^{m+\tau+1} \tag{13}$$

Thus, to leading order the exponent increases from τ to $(m + \tau)$ if a piecewise-constant cloud is replaced by one with a m-th degree polynomial flank. Note this indicates that by examining projections, one cannot distinguish between local gradients of density and the local shape of the boundary curve of the cloud.

3. POWER SPECTRAL DENSITIES OF PIECEWISE-CONSTANT CLOUDS AND PROJECTIONS

3.1 Clouds

We define the direct and inverse Fourier transforms of an n-dimensional cloud as

$$\hat{f}(\underset{\sim}{k}) \equiv \hat{f}(k_1, k_2, \ldots, k_n) = \int_{(n)} f(\underset{\sim}{x}) e^{-i\underset{\sim}{k}\cdot\underset{\sim}{x}} d\underset{\sim}{x} \ , \ \underset{\sim}{x} \in \mathbb{R}^n \tag{14}$$

$$f(\underset{\sim}{x}) = f(x_1, x_2, \ldots, x_n) = (2\pi)^{-n} \int_{(n)} \hat{f}(\underset{\sim}{k}) e^{+i\underset{\sim}{k}\cdot\underset{\sim}{x}} d\underset{\sim}{k} \ , \ \underset{\sim}{k} \in \mathbb{R}^n \tag{15}$$

where $\int_{(n)}$ symbolizes n integrations that cover the entire domain and $d\underset{\sim}{x} \equiv dx_1\, dx_2 \ldots dx_n$ and $d\underset{\sim}{k} \equiv dk_1\, dk_2 \ldots dk_n$. The last can be written as $d\underset{\sim}{k} = dk\, d\sigma_k$, where $k = |\underset{\sim}{k}|$ and $d\sigma_k$ is an (n-1)-dimensional surface differential such that $\int_{(n-1)} d\sigma_k = 2\pi^{n/2}/\Gamma(n/2)$. The functions f and $\hat{f}$ satisfy Parseval's formula

$$E_T \equiv \int |\hat{f}|^2\, d\underset{\sim}{k} = (2\pi)^n \int |f(\underset{\sim}{x})|^2\, d\underset{\sim}{x}, \tag{16}$$

where $|\hat{f}|^2$ is the PSD.

Gelfand et al.[5] show that if the boundary ∂D of a pc cloud of density F_0 is a convex surface (i.e., at each point on ∂D the product of the principal radii of curvature $\neq 0$), and if ∂D is centrally symmetric about the origin (e.g., like an ellipsoid), then the asymptotic spectrum is

$$\hat{f}(\underset{\sim}{k}) = 2F_0(2\pi)^{(n-1)/2}\{\rho_1\rho_2\cdots\rho_{n-1}\}^{(1/2)}k^{-(n+1)/2}$$

$$\times \cos\left[k\hat{a} - \frac{1}{4}(n+1)\pi\right]\{1 + O\{k^{-1/2}\}\}, \tag{17}$$

where $k = |\underset{\sim}{k}|$, $2\hat{a}$ is the "diameter" of D perpendicular to the direction $\underset{\sim}{k}/k$ (which is associated with the index n) and $\rho_1, \rho_2, \ldots, \rho_{n-1}$ are the principal radii of curvature at points A and A′ on ∂D, namely the extremal points. Figure 3 illustrates these quantities for an ellipse ($n = 2$) where $\underset{\sim}{k}/k = \underset{\sim}{e}_y$, and the curvatures $\kappa = 1/\rho_1$ at A and A′ are the same, since the ellipse is centrally symmetric. The two-dimensional PSD obtained from (17) is

$$E(k) \equiv |\hat{f}(k)|^2 = 8\pi F_0^2\rho_1 k^{-3}\cos^2\left[k\hat{a} - \frac{3\pi}{4}\right]\{1 + O\{k^{-1/2}\}\}. \tag{18}$$

We define the one-dimensional PSD as

$$E_1(k) \equiv k^{n-1}\int_{(n-1)} d\sigma_k\, E(\underset{\sim}{k}) = k^{n-1}\int_{(n-1)} d\sigma_k |\hat{f}|^2, \tag{19}$$

and thus $E_T = \int_{-\infty}^{+\infty} dk\, E_1(k)$. From (19) with (17) the dominant term in $E_1(k)$ is

$$E_1(k) = \left[2^{n+2}\pi^{\{\frac{3n}{2} - 1\}}/\Gamma\{\tfrac{n}{2}\}\right]F_0^2 k^{-2}\{\rho_1\rho_2\cdots\rho_{n-1}\}\cos^2\left[k\hat{a} - \frac{1}{4}(n+1)\pi\right] + \ldots \tag{20}$$

That is, the asymptotic dependence of the one-dimensional PSD of an n-dimensional <u>piecewise</u> <u>constant</u> cloud with convex boundaries is proportional to k^{-2} and the quantity in brackets is $(4\pi)^2$ or $(4\pi)^3$ for $n = 2$ or 3, respectively. The amplitude of the asymptotic spectrum is inversely proportional to the product of the <u>curvatures</u> at the extremal points.

3.2 Projections

In Section 2 we have shown that in a small region near the tangent ray (e.g., the origin $x = 0$), we can represent the projection function as

$$f(x) = x^{\tau}h(x),\ x > 0, \tag{21}$$

where $h(x)$ is an analytic function for $x > 0$ and $\tau > 0$. The simplest projection function for a convex cloud is

$$f(x) = x^{\tau_1}[1 - (x/a_2)]^{\tau_2} h_{12}(x), \quad 0 < x < a_2,$$

where h_{12} is analytic and greater than zero between $0 < x < a_2$, and τ_1, τ_2 are > 0. The asymptotic spectrum will depend on which exponent is most singular, that is, smaller. For simplicity, we consider one such point and examine the Fourier transform

$$\hat{f}(k) = \int_0^\infty e^{-ikx} x^\tau h(x)\, dx$$

or

$$\hat{f}(k) = k^{-(\tau+1)} \int_0^\infty e^{-i\xi} \xi^\tau h(\xi/k) d\xi \tag{22}$$

where $kx = \xi$. If one applies the method of stationary phase[6] for $k >> 1$ we can show that the integral is $O(1)$ and the asymptotic spectral index of $\hat{f}$ is $-(\tau + 1)$. The result agrees with that presented in our previous report,[3] namely for the function

$$\begin{gathered} f = 1,\ |x| < a,\ f = 0,\ |x| > b \\ f = [1 - (x-a)^2(b-a)^{-2}]^\tau,\ a < |x| < b, \end{gathered} \tag{23}$$

the asymptotic spectrum is $-(\tau + 1)$ or the spectral index of the PSD of f is $p = 2(\tau + 1)$.

We conclude with the results: For clouds contained in a finite domain and having a polynomial flank of degree m (see Equation (11)), the asymptotic spectral index of $|\hat{f}|^2$ (the PSD of the projection function f(x)) is

$$p = 2(1 + \tau + m).$$

For pc densities ($m = 0$) the asymptotic spectral behavior is given in the last column of Table 1. Note the well-known result, a k^{-3} dependence occurs when the curvature at the extremal ray is finite ($\tau = 1/2$). Furthermore, the asymptotic spectral index varies continuously from slightly greater than 2 ($\tau = \epsilon$) to indefinitely large values depending upon the nature of the cusp. Note, a linear flank on a convex curve gives an asymptotic PSD α k^{-5}.

4. APPLICATION OF RESULTS

We apply the results of the present and previous[3] papers to data from the recent "PLACES" high-altitude barium cloud releases.[7] We will show that the PSD results in Reference 7 for events GAIL and IRIS are valid only for the small wavenumber region, $K < 1.5$ km^{-1} which is the region associated with the mean size of the cloud. These spectra do not yield any information about the asymptotic spectral index. Such exponents arise in a Rufenach fit to a nonlinear dynamical process, namely

$$\mathrm{PSD}(K) = [1 + (KL_o)^2]^{-p/2}$$

where $(KL_o) \gg 1$. In this section K = radians/km = (length)$^{-1}$ (i.e. not the conventional 2π/(length)) and L_o is the outer scale length, typically 1 km to 3 km.

Optical emission data for events GAIL and IRIS are given in reference 7 in several forms: non field-aligned photographs of optical emission; smoothed optical radiance contours (e.g., Fig. 4a and 5a); several scans of the contours in a direction transverse to the local magnetic field (e.g. Fig. 4b and 5b); and a PSD of a "windowed" scan (e.g. Fig. 4c and 5c). Several features of the data reduction process deserve comment.[8] In windowing, the given data is multiplied by a prescribed function (a Kaiser-Bessel window) which makes the resulting function nearly periodic. This avoids discontinuities and large contributions to the high-wave number spectrum at the expense of introducing a frequency domain "smoothing" by convolution.[9] In Figs. 4a and 5a three rectangular regions are shown. The scans or profiles in Figs. 4b and 5b and their standard deviations are obtained by averaging 21 separate scans in each rectangular region. Typically this involves fewer than $256\sqrt{2} \approx 362$ points per scan. This data is then reinterpolated with 250 to 500 points (twice the ratio of the highest to the lowest mode number) so as to obtain a reasonable fit to the oscillations, which are attributed to striations. These reasonable but ad hoc procedures lead one to question the validity of the highest 50% of the modes as a representation of the nonlinear dynamics of striation evolution. The following table presents pertinent information obtained from the small figures in Ref. 7.

FIG.	EVENT	REF. 7	HIGHEST MODE (km^{-1})	LOWEST MODE (km^{-1})	HIGHEST MODE / LOWEST MODE	EST. SPECTRAL INDEX (REF. 7)
4C	IRIS	FIG. 66 (LOWEST)	6.6	0.066	100	2.5
5C	GAIL	FIG. 51 (LOWEST)	7.6	0.038	200	2.5

For an approximation consistent with the location of the first two nulls, the data in Figures 4c and 5c are conveniently fit with trapezoids. For example, the symmetric trapezoid with altitude A, upper and lower parallel sides 2a and 2b, respectively, has a PSD[3]

$$|\hat{f}|^2 = \lfloor A(b + a)\ (\sin z_+ \sin z_-)/(z_+ z_-)\rfloor^2 ,$$

where

$$z_{\pm} = \pi K(b \pm a).$$

Thus, if the scales are well-separated, $(b + a)/(b - a) \gg 1$, then we have a k^{-2} envelope for $K_{11} \equiv 2/(b + a) < K < K_{21} \equiv 2/(b - a)$ and a k^{-4} envelope for $K > K_{21}$. From our asymptotic theory given in Section 2, the k^{-4} region would occur, no matter what the shape of the function in the region $(b - a)$, where the trapezoid is linear. This linear behavior corresponds to $\tau = 1$ in Table 1. If other exponents, τ , describe the function in this narrow region then the appropriate spectral index envelope would be $2(\tau + 1)$.

The first two nulls in Fig. 4c are consistent with fitting the scan in Fig. 4b with a symmetrical trapezoid whose upper and lower parallel sides are $2a = 1.8$ km and $2b = 6.2$ km. The first null of the discrete Fourier transform, $K_{11} = 2/(b + a) = 0.5$ is associated with the first transition. The first null of the second transition is at $K_{21} = 2/(b-a) = 1.1$ and is consistent with the second null in Fig. 4c. Hence we conclude that the scales are not well separated. The only information available concerning the asymptotic spectrum lies in the range $K > 1.5$. This region represents a composite of effects resulting from: the K^{-4} trapezoidal spectrum; the small-scale structures on the trapezoid (their widths and separations); film grain noise; and aliasing. One cannot see the spectral index of individual striations.

Event GAIL had steeper gradients as shown in Fig. 5b. One could approximate this scan function by an unsymmetric trapezoid with an upper parallel side $2a = 14.5$ km and a base composed of a right segment $b_1 = 8.45$ km and a left segment $b_2 = 9.45$ km. The lack of symmetry causes an interference of the nulls and they aren't as clean as in the discussion of Fig. 4b. However, it is reasonable to approximate the unsymmetric trapezoid with a symmetric one with $2b = 17.9$ then $K_{11} = 0.123$ and $K_{21} = 1.18$, a good separation of scales. Thus, between 0.123 and 1.18 the spectral index is changing from 2 to 4. For $K > 1.2$ a comment similar to that given in the above paragraph applies.

As discussed in reference 3, to make a good esimate of the asymptotic spectral index from a scan with no noise, one needs at least:

256 modes	for a scan function with two k-space regions
10,000 modes	for a scan function with three well separated k-space regions.

Thus, we conclude the data presented do not allow one to deduce the spectral index of striations. It is obvious that a single unqualified PSD index can be misleading.

5. CONCLUSIONS

In this report we have considered the relationship between a radiating cloud and the power spectral density of a scan of its photographic image. To allow us to focus on the uncertainties associated with geometrical aspects, we have assumed idealized conditions, namely: optically thin clouds, no parallax effects and no distortion due to camera, lenses and film grain.. We have considered clouds with a piecewise constant and power law radiating density. We have not attempted to correlate this radiant density with the ion density.

For convex piecewise-constant clouds, where the one-dimensional asymptotic spectrum of the power is proportional to k^{-2}, we have shown that the asymptotic spectrum of the scan depends upon the character of the contour at the point where it is tangent to the extremal ray. If the contour at (x_0, y_0) behaves like $y - y_0 = \gamma(x - x_0)^{\tau}$ then the asymptotic spectral envelope of the PSD of the scan varies as $k^{-2(\tau + 1)}$. In addition, if the radiating density in a cloud flank varies with a power law m then the asymptotic spectral envelope of the scan's PSD varies as $k^{-2(1 + \tau + m)}$.

We have applied these considerations to data from PLACES events IRIS and GAIL. We have shown that the spectral index obtained in Ref. 8 is associated with a fit to an intermediate region with several competing effects and is not associated with the asymptotic spectral index that arises in nonlinear turbulent or wave steepening dynamical processes.

ACKNOWLEDGMENTS

We are grateful to L. Testerman of EG&G for help in interpreting the data analysis procedures in Refs. 7 and 8. We also acknowledge constructive remarks by W. Chesnut and C. Rino of SRI. This work was supported by the Defense Nuclear Agency.

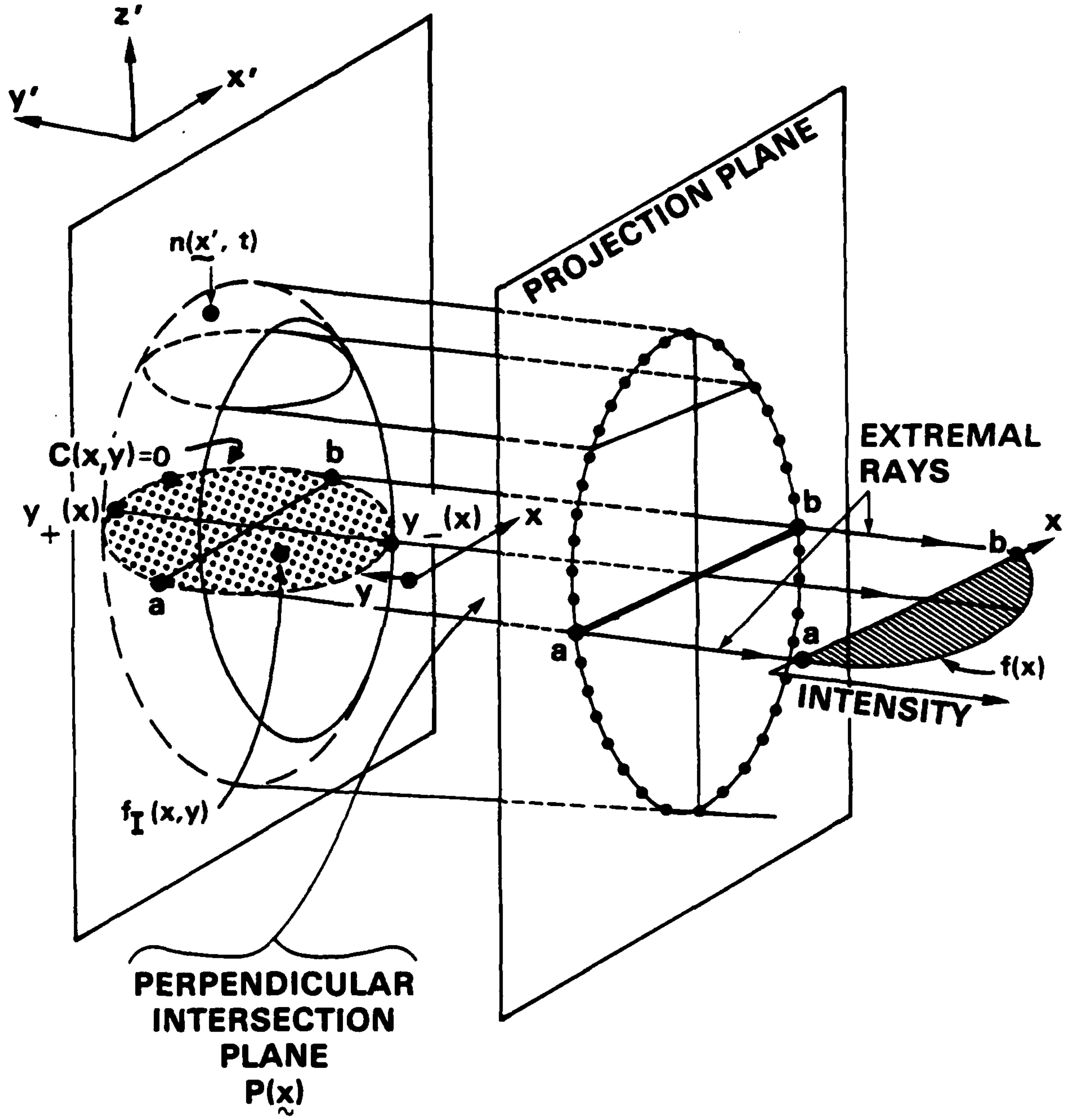

Fig. 1 — Schematic of a remote radiating cloud and the projection function f(x) through a slice of the cloud

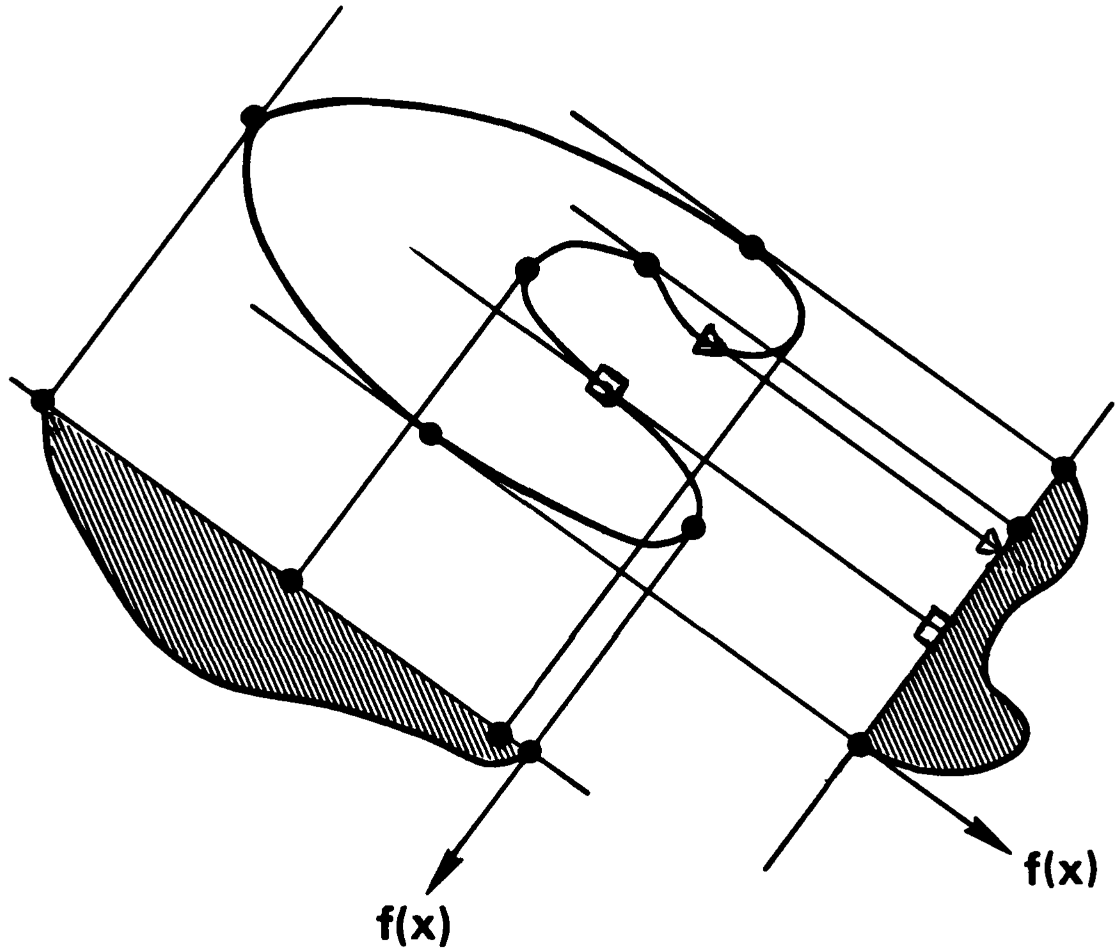

Fig. 2 — Two projections of a realistic two-finger cloud showing the effects of tangency points (□ and Δ) where $\kappa = 0$

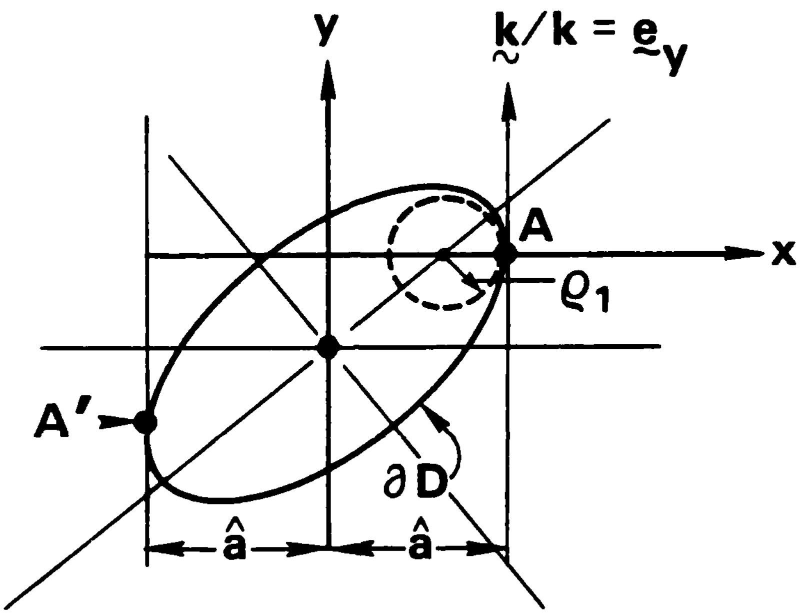

Fig. 3 — Parameters used to define the asymptotic spectrum of a convex centrally symmetric piecewise-constant 2D cloud

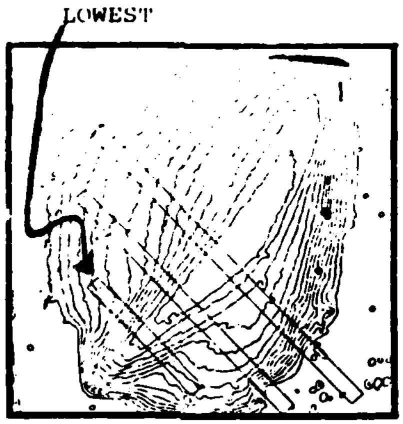

(a) Smoothed radiance contours and three rectangular regions in which scans are made

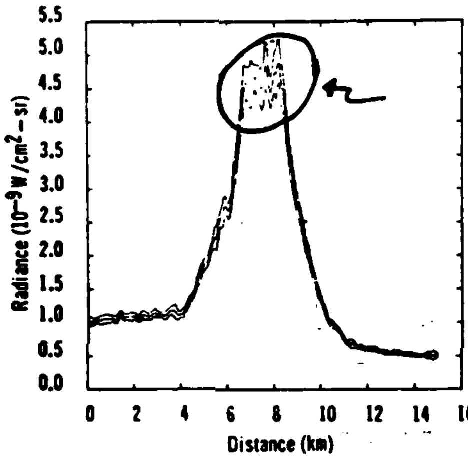

(b) Fitted radiance profiles with upper and lower standard deviation corresponding to the lowest scanning rectangle. Small scale oscillations in arrowed circle indicate striations. (These are resolved with about 10 points per period.)

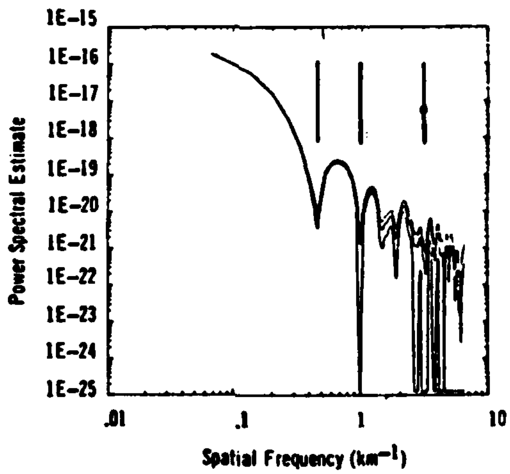

(c) PSD of information in (b) above after using a Kaiser-Bessel window

Fig. 4 — Event IRIS. PSD contains 100 modes. (Reference 7, Figures 65 and 66)

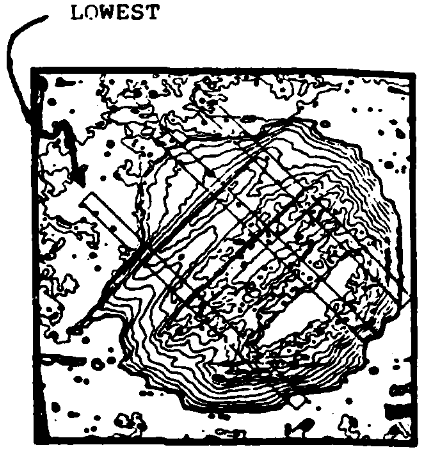

(a) Smoothed radiance contours and three rectangular regions in which scans are made

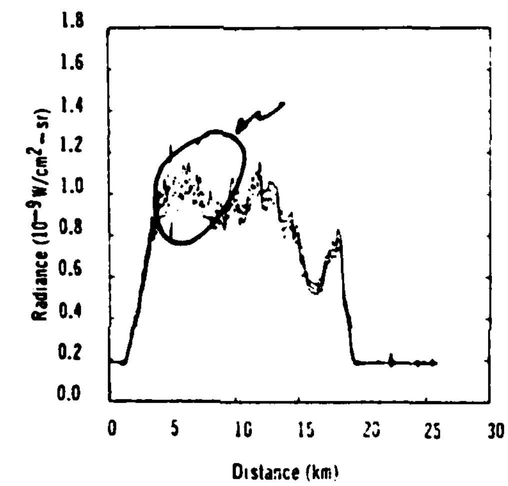

(b) Fitted radiance profiles with upper and lower standard deviation corresponding to the lowest scanning rectangle. Small scale oscillations in arrowed circle indicate striations. (These are resolved with about 10 points per period.)

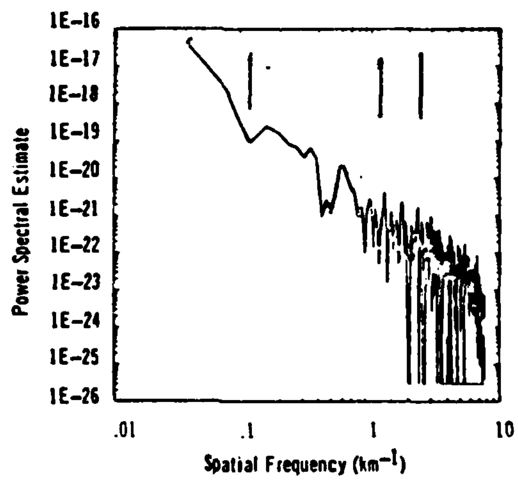

(c) PSD of information in (b) above after using a Kaiser-Bessel window

Fig. 5 — EVENT GAIL. PSD contains 200 modes. (Reference 7, Figures 50 and 51)

REFERENCES

1. L.A. Shepp and J.B. Kruskal, Computerized tomography: the new medical x-ray technology, Amer. Math. Monthly, 85 420-439, June-July, 1978.
2. S.R. Deans, The Radon transform and some of its applications, Wiley, New York, 1983.
3. M. Mulbrandon, N.J. Zabusky and E. Hyman, Estimating Spectral Indices from Transforms of Discrete Representations of Density Functions, NRL Memo Report No. 5298, 1984.(AD-A140164)
4. C. Lebeda, S.P. Gary, and M.B. Pongratz, Density Spectra as a Function of Altitude in an Ionospheric Barium Release," Geophys. Res. Lett. 11, 591-594, 1984.
5. I.M. Gelfand, M.I. Graev, N. Ya. Vilenkin, Generalized Functions, Vol. 5, Integral Geometry and Representation Theory. Academic Press, NY, 1966. See Sec. 1.7, p. 19.
6. F.W.J. Olver, Asymptotics and Special Functions, Academic Press, NY, 1974. The method of stationary phase is discussed in Section 11 and theorems for finite range Fourier transforms are given in Section 13. The Riemann-Lebesgue lemma, discussed in Sec 4.2, plays an important role in obtaining these asymptotic results.
7. D.J. Simons, C.F. Lebeda, M.B. Pongratz, T.J. Fitzgerald, R.R. Dupre, Evolution of Structure in the PLACES Barium Clouds, Los Alamos National Laboratory LA 9648-MS, February 1984.
8. The procedures for transforming the photographs into PSD are described in C.F. Lebeda, "Procedures for analysis of photographic records of striated clouds," EGG report No. EGG 10282-5008, June 1983. In a telephone conversation (8/27/84), L. Testerman of EGG described pertinent numbers. The smoothed radiance contours were obtained from a 256 x 256 digitization of a selected portion of a 35 mm frame. To obtain the fitted radiance profiles with deviations (3 curves), 21 scans were made in each rectangular region and averaged. Each profile was then digitized with 250-500 points (125-250 modes) depending on the resolution of the small scale oscillations which are attributed to striations. Usually 7 to 10 points per oscillation was considered "reasonable".
9. F.J. Harris, On the use of windows for harmonic analysis with the discrete Fourier transform, Proc. IEEE, 66, 51-83, 1978.

DISTRIBUTION LIST

DEPARTMENT OF DEFENSE

ASSISTANT SECRETARY OF DEFENSE
COMM, CMD, CONT 7 INTELL
WASHINGTON, D.C. 20301

DIRECTOR
COMMAND CONTROL TECHNICAL CENTER
PENTAGON RM BE 685
WASHINGTON, D.C. 20301
01CY ATTN C-650
01CY ATTN C-312 R. MASON

DIRECTOR
DEFENSE ADVANCED RSCH PROJ AGENCY
ARCHITECT BUILDING
1400 WILSON BLVD.
ARLINGTON, VA. 22209
01CY ATTN NUCLEAR MONITORING RESEARCH
01CY ATTN STRATEGIC TECH OFFICE

DEFENSE COMMUNICATION ENGINEER CENTER
1860 WIEHLE AVENUE
RESTON, VA. 22090
01CY ATTN CODE R410
01CY ATTN CODE R812

DEFENSE TECHNICAL INFORMATION CENTER
CAMERON STATION
ALEXANDRIA, VA. 22314
02CY

DIRECTOR
DEFENSE NUCLEAR AGENCY
WASHINGTON, D.C. 20305
01CY ATTN STVL
04CY ATTN TITL
01CY ATTN DDST
03CY ATTN RAAE

COMMANDER
FIELD COMMAND
DEFENSE NUCLEAR AGENCY
KIRTLAND, AFB, NM 87115
01CY ATTN FCPR

DEFENSE NUCLEAR AGENCY
SAO/DNA
BUILDING 20676
KIRTLAND AFB, NM 87115
01CY D.C. THORNBURG

DIRECTOR
INTERSERVICE NUCLEAR WEAPONS SCHOOL
KIRTLAND AFB, NM 87115
01CY ATTN DOCUMENT CONTROL

JOINT CHIEFS OF STAFF
WASHINGTON, D.C. 20301
01CY ATTN J-3 WWMCCS EVALUATION OFFICE

DIRECTOR
JOINT STRAT TGT PLANNING STAFF
OFFUTT AFB
OMAHA, NB 68113
01CY ATTN JSTPS/JLKS
01CY ATTN JPST G. GOETZ

CHIEF
LIVERMORE DIVISION FLD COMMAND DNA
DEPARTMENT OF DEFENSE
LAWRENCE LIVERMORE LABORATORY
P.O. BOX 808
LIVERMORE, CA 94550
01CY ATTN FCPRL

COMMANDANT
NATO SCHOOL (SHAPE)
APO NEW YORK 09172
01CY ATTN U.S. DOCUMENTS OFFICER

UNDER SECY OF DEF FOR RSCH & ENGRG
DEPARTMENT OF DEFENSE
WASHINGTON, D.C. 20301
01CY ATTN STRATEGIC & SPACE SYSTEMS (OS)

WWMCCS SYSTEM ENGINEERING ORG
WASHINGTON, D.C. 20305
01CY ATTN R. CRAWFORD

COMMANDER/DIRECTOR
ATMOSPHERIC SCIENCES LABORATORY
U.S. ARMY ELECTRONICS COMMAND
WHITE SANDS MISSILE RANGE, NM 88002
01CY ATTN DELAS-EO, F. NILES

DIRECTOR
BMD ADVANCED TECH CTR
HUNTSVILLE OFFICE
P.O. BOX 1500
HUNTSVILLE, AL 35807
01CY ATTN ATC-T MELVIN T. CAPPS
01CY ATTN ATC-O W. DAVIES
01CY ATTN ATC-R DON RUSS

PROGRAM MANAGER
BMD PROGRAM OFFICE
5001 EISENHOWER AVENUE
ALEXANDRIA, VA 22333
01CY ATTN DACS-BMT J. SHEA

CHIEF C-E- SERVICES DIVISION
U.S. ARMY COMMUNICATIONS CMD
PENTAGON RM 1B269
WASHINGTON, D.C. 20310
01CY ATTN C- E-SERVICES DIVISION

COMMANDER
FRADCOM TECHNICAL SUPPORT ACTIVITY
DEPARTMENT OF THE ARMY
FORT MONMOUTH, N.J. 07703
01CY ATTN DRSEL-NL-RD H. BENNET
01CY ATTN DRSEL-PL-ENV H. BOMKE
01CY ATTN J.E. QUIGLEY

COMMANDER
U.S. ARMY COMM-ELEC ENGRG INSTAL AGY
FT. HUACHUCA, AZ 85613
01CY ATTN CCC-EMEO GEORGE LANE

COMMANDER
U.S. ARMY FOREIGN SCIENCE & TECH CTR
220 7TH STREET, NE
CHARLOTTESVILLE, VA 22901
01CY ATTN DRXST-SD

COMMANDER
U.S. ARMY MATERIAL DEV & READINESS CMD
5001 EISENHOWER AVENUE
ALEXANDRIA, VA 22333
01CY ATTN DRCLDC J.A. BENDER

COMMANDER
U.S. ARMY NUCLEAR AND CHEMICAL AGENCY
7500 BACKLICK ROAD
BLDG 2073
SPRINGFIELD, VA 22150
01CY ATTN LIBRARY

DIRECTOR
U.S. ARMY BALLISTIC RESEARCH
LABORATORY
ABERDEEN PROVING GROUND, MD 21005
01CY ATTN TECH LIBRARY,
EDWARD BAICY

COMMANDER
U.S. ARMY SATCOM AGENCY
FT. MONMOUTH, NJ 07703
01CY ATTN DOCUMENT CONTROL

COMMANDER
U.S. ARMY MISSILE INTELLIGENCE AGENCY
REDSTONE ARSENAL, AL 35809
01CY ATTN JIM GAMBLE

DIRECTOR
U.S. ARMY TRADOC SYSTEMS ANALYSIS
ACTIVITY
WHITE SANDS MISSILE RANGE, NM 88002
01CY ATTN ATAA-SA
01CY ATTN TCC/F. PAYAN JR.
01CY ATTN ATTA-TAC LTC J. HESSE

COMMANDER
NAVAL ELECTRONIC SYSTEMS COMMAND
WASHINGTON, D.C. 20360
01CY ATTN NAVALEX 034 T. HUGHES
01CY ATTN PME 117
01CY ATTN PME 117-T
01CY ATTN CODE 5011

COMMANDING OFFICER
NAVAL INTELLIGENCE SUPPORT CTR
4301 SUITLAND ROAD, BLDG. 5
WASHINGTON, D.C. 20390
01CY ATTN MR. DUBBIN STIC 12
01CY ATTN NISC-50
01CY ATTN CODE 5404 J. GALET

COMMANDER
NAVAL OCCEAN SYSTEMS CENTER
SAN DIEGO, CA 92152
01CY ATTN J. FERGUSON

NAVAL RESEARCH LABORATORY
WASHINGTON, D.C. 20375
01CY ATTN CODE 4700 S. L. Ossakow 26 CYS IF UNCLASS. 1 CY IF CLASS)
01CY ATTN CODE 4701 I Vitkovitsky
01CY ATTN CODE 4780 J. Huba (100 CYS IF UNCLASS, 1 CY IF CLASS)
01CY ATTN CODE 7500
01CY ATTN CODE 7550
01CY ATTN CODE 7580
01CY ATTN CODE 7551
01CY ATTN CODE 7555
01CY ATTN CODE 4730 E. MCLEAN
01CY ATTN CODE 4108
01CY ATTN CODE 4730 B. RIPIN
20CY ATTN CODE 2628

COMMANDER
NAVAL SPACE SURVEILLANCE SYSTEM
DAHLGREN, VA 22448
01CY ATTN CAPT J.H. BURTON

OFFICER-IN-CHARGE
NAVAL SURFACE WEAPONS CENTER
WHITE OAK, SILVER SPRING, MD 20910
01CY ATTN CODE F31

DIRECTOR
STRATEGIC SYSTEMS PROJECT OFFICE
DEPARTMENT OF THE NAVY
WASHINGTON, D.C. 20376
01CY ATTN NSP-2141
01CY ATTN NSSP-2722 FRED WIMBERLY

COMMANDER
NAVAL SURFACE WEAPONS CENTER
DAHLGREN LABORATORY
DAHLGREN, VA 22448
01CY ATTN CODE DF-14 R. BUTLER

OFFICER OF NAVAL RESEARCH
ARLINGTON, VA 22217
01CY ATTN CODE 465
01CY ATTN CODE 461
01CY ATTN CODE 402
01CY ATTN CODE 420
01CY ATTN CODE 421

COMMANDER
AEROSPACE DEFENSE COMMAND/DC
DEPARTMENT OF THE AIR FORCE
ENT AFB, CO 80912
01CY ATTN DC MR. LONG

COMMANDER
AEROSPACE DEFENSE COMMAND/XPD
DEPARTMENT OF THE AIR FORCE
ENT AFB, CO 80912
01CY ATTN XPDQQ
01CY ATTN XP

AIR FORCE GEOPHYSICS LABORATORY
HANSCOM AFB, MA 01731
01CY ATTN OPR HAROLD GARDNER
01CY ATTN LKB KENNETH S.W. CHAMPION
01CY ATTN OPR ALVA T. STAIR
01CY ATTN PHD JURGEN BUCHAU
01CY ATTN PHD JOHN P. MULLEN

AF WEAPONS LABORATORY
KIRTLAND AFT, NM 87117
01CY ATTN SUL
01CY ATTN CA ARTHUR H. GUENTHER
01CY ATTN NTYCE 1LT. G. KRAJEI

AFTAC
PATRICK AFB, FL 32925
01CY ATTN TN

AIR FORCE AVIONICS LABORATORY
WRIGHT-PATTERSON AFB, OH 45433
01CY ATTN AAD WADE HUNT
01CY ATTN AAD ALLEN JOHNSON

DEPUTY CHIEF OF STAFF
RESEARCH, DEVELOPMENT, & ACQ
DEPARTMENT OF THE AIR FORCE
WASHINGTON, D.C. 20330
01CY ATTN AFRDQ

HEADQUARTERS
ELECTRONIC SYSTEMS DIVISION
DEPARTMENT OF THE AIR FORCE
HANSCOM AFB, MA 01731
01CY ATTN J. DEAS

HEADQUARTERS
ELECTRONIC SYSTEMS DIVISION/YSEA
DEPARTMENT OF THE AIR FORCE
HANSCOM AFB, MA 01732
01CY ATTN YSEA

HEADQUARTERS
ELECTRONIC SYSTEMS DIVISION/DC
DEPARTMENT OF THE AIR FORCE
HANSCOM AFB, MA 01731
01CY ATTN DCKC MAJ J.C. CLARK

COMMANDER
FOREIGN TECHNOLOGY DIVISION, AFSC
WRIGHT-PATTERSON AFB, OH 45433
01CY ATTN NICD LIBRARY
01CY ATTN ETDP B. BALLARD

COMMANDER
ROME AIR DEVELOPMENT CENTER, AFSC
GRIFFISS AFB, NY 13441
01CY ATTN DOC LIBRARY/TSLD
01CY ATTN OCSE V. COYNE

SAMSO/SZ
POST OFFICE BOX 92960
WORLDWAY POSTAL CENTER
LOS ANGELES, CA 90009
(SPACE DEFENSE SYSTEMS)
01CY ATTN SZJ

STRATEGIC AIR COMMAND/XPFS
OFFUTT AFB, NB 68113
01CY ATTN ADWATE MAJ BRUCE BAUER
01CY ATTN NRT
01CY ATTN DOK CHIEF SCIENTIST

SAMSO/SK
P.O. BOX 92960
WORLDWAY POSTAL CENTER
LOS ANGELES, CA 90009
01CY ATTN SKA (SPACE COMM SYSTEMS) M. CLAVIN

SAMSO/MN
NORTON AFB, CA 92409
(MINUTEMAN)
01CY ATTN MNNL

COMMANDER
ROME AIR DEVELOPMENT CENTER, AFSC
HANSCOM AFB, MA 01731
01CY ATTN EEP A. LORENTZEN

DEPARTMENT OF ENERGY
LIBRARY ROOM G-042
WASHINGTON, D.C. 20545
01CY ATTN DOC CON FOR A. LABOWITZ

DEPARTMENT OF ENERGY
ALBUQUERQUE OPERATIONS OFFICE
P.O. BOX 5400
ALBUQUERQUE, NM 87115
01CY ATTN DOC CON FOR D. SHERWOOD

EG&G, INC.
LOS ALAMOS DIVISION
P.O. BOX 809
LOS ALAMOS, NM 85544
01CY ATTN DOC CON FOR J. BREEDLOVE

UNIVERSITY OF CALIFORNIA
LAWRENCE LIVERMORE LABORATORY
P.O. BOX 808
LIVERMORE, CA 94550
01CY ATTN DOC CON FOR TECH INFO DEPT
01CY ATTN DOC CON FOR L-389 R. OTT
01CY ATTN DOC CON FOR L-31 R. HAGER

LOS ALAMOS NATIONAL LABORATORY
P.O. BOX 1663
LOS ALAMOS, NM 87545
01CY ATTN DOC CON FOR J. WOLCOTT
01CY ATTN DOC CON FOR R.F. TASCHEK
01CY ATTN DOC CON FOR E. JONES
01CY ATTN DOC CON FOR J. MALIK
01CY ATTN DOC CON FOR R. JEFFRIES
01CY ATTN DOC CON FOR J. ZINN
01CY ATTN DOC CON FOR P. KEATON
01CY ATTN DOC CON FOR D. WESTERVELT
01CY ATTN D. SAPPENFIELD

SANDIA LABORATORIES
P.O. BOX 5800
ALBUQUERQUE, NM 87115
01CY ATTN DOC CON FOR W. BROWN
01CY ATTN DOC CON FOR A. THORNBROUGH
01CY ATTN DOC CON FOR T. WRIGHT
01CY ATTN DOC CON FOR D. DAHLGREN
01CY ATTN DOC CON FOR 3141
01CY ATTN DOC CON FOR SPACE PROJECT DIV

SANDIA LABORATORIES
LIVERMORE LABORATORY
P.O. BOX 969
LIVERMORE, CA 94550
01CY ATTN DOC CON FOR B. MURPHEY
01CY ATTN DOC CON FOR T. COOK

OFFICE OF MILITARY APPLICATION
DEPARTMENT OF ENERGY
WASHINGTON, D.C. 20545
01CY ATTN DOC CON DR. YO SONG

OTHER GOVERNMENT

INSTITUTE FOR TELECOM SCIENCES
NATIONAL TELECOMMUNICATIONS & INFO ADMIN
BOULDER, CO 80303
01CY ATTN A. JEAN (UNCLASS ONLY)
01CY ATTN W. UTLAUT
01CY ATTN D. CROMBIE
01CY ATTN L. BERRY

NATIONAL OCEANIC & ATMOSPHERIC ADMIN
ENVIRONMENTAL RESEARCH LABORATORIES
DEPARTMENT OF COMMERCE
BOULDER, CO 80302
01CY ATTN R. GRUBB
01CY ATTN AERONOMY LAB G. REID

DEPARTMENT OF DEFENSE CONTRACTORS

AEROSPACE CORPORATION
P.O. BOX 92957
LOS ANGELES, CA 90009
01CY ATTN I. GARFUNKEL
01CY ATTN T. SALMI
01CY ATTN V. JOSEPHSON
01CY ATTN S. BOWER
01CY ATTN D. OLSEN

ANALYTICAL SYSTEMS ENGINEERING CORP
5 OLD CONCORD ROAD
BURLINGTON, MA 01803
01CY ATTN RADIO SCIENCES

AUSTIN RESEARCH ASSOC., INC.
1901 RUTLAND DRIVE
AUSTIN, TX 78758
01CY ATTN L. SLOAN
01CY ATTN R. THOMPSON

BERKELEY RESEARCH ASSOCIATES, INC.
P.O. BOX 983
BERKELEY, CA 94701
01CY ATTN J. WORKMAN
01CY ATTN C. PRETTIE
01CY ATTN S. BRECHT

BOEING COMPANY, THE
P.O. BOX 3707
SEATTLE, WA 98124
01CY ATTN G. KEISTER
01CY ATTN D. MURRAY
01CY ATTN G. HALL
01CY ATTN J. KENNEY

CHARLES STARK DRAPER LABORATORY, INC.
555 TECHNOLOGY SQUARE
CAMBRIDGE, MA 02139
01CY ATTN D.B. COX
01CY ATTN J.P. GILMORE

COMSAT LABORATORIES
LINTHICUM ROAD
CLARKSBURG, MD 20734
01CY ATTN G. HYDE

CORNELL UNIVERSITY
DEPARTMENT OF ELECTRICAL ENGINEERING
ITHACA, NY 14850
01CY ATTN D.T. FARLEY, JR.

ELECTROSPACE SYSTEMS, INC.
BOX 1359
RICHARDSON, TX 75080
01CY ATTN H. LOGSTON
01CY ATTN SECURITY (PAUL PHILLIPS)

EOS TECHNOLOGIES, INC.
606 Wilshire Blvd.
Santa Monica, Calif 90401
01CY ATTN C.B. GABBARD
01CY ATTN R. LELEVIER

ESL, INC.
495 JAVA DRIVE
SUNNYVALE, CA 94086
01CY ATTN J. ROBERTS
01CY ATTN JAMES MARSHALL

GENERAL ELECTRIC COMPANY
SPACE DIVISION
VALLEY FORGE SPACE CENTER
GODDARD BLVD KING OF PRUSSIA
P.O. BOX 8555
PHILADELPHIA, PA 19101
01CY ATTN M.H. BORTNER SPACE SCI LAB

GENERAL ELECTRIC COMPANY
P.O. BOX 1122
SYRACUSE, NY 13201
01CY ATTN F. REIBERT

GENERAL ELECTRIC TECH SERVICES CO., INC.
HMES
COURT STREET
SYRACUSE, NY 13201
01CY ATTN G. MILLMAN

GEOPHYSICAL INSTITUTE
UNIVERSITY OF ALASKA
FAIRBANKS, AK 99701
(ALL CLASS ATTN: SECURITY OFFICER)
01CY ATTN T.N. DAVIS (UNCLASS ONLY)
01CY ATTN TECHNICAL LIBRARY
01CY ATTN NEAL BROWN (UNCLASS ONLY)

GTE SYLVANIA, INC.
ELECTRONICS SYSTEMS GRP-EASTERN DIV
77 A STREET
NEEDHAM, MA 02194
01CY ATTN DICK STEINHOF

HSS, INC.
2 ALFRED CIRCLE
BEDFORD, MA 01730
01CY ATTN DONALD HANSEN

ILLINOIS, UNIVERSITY OF
107 COBLE HALL
150 DAVENPORT HOUSE
CHAMPAIGN, IL 61820
(ALL CORRES ATTN DAN MCCLELLAND)
01CY ATTN K. YEH

INSTITUTE FOR DEFENSE ANALYSES
1801 NO. BEAUREGARD STREET
ALEXANDRIA, VA 22311
01CY ATTN J.M. AEIN
01CY ATTN ERNEST BAUER
01CY ATTN HANS WOLFARD
01CY ATTN JOEL BENGSTON

INTL TEL & TELEGRAPH CORPORATION
500 WASHINGTON AVENUE
NUTLEY, NJ 07110
01CY ATTN TECHNICAL LIBRARY

JAYCOR
11011 TORREYANA ROAD
P.O. BOX 85154
SAN DIEGO, CA 92138
01CY ATTN J.L. SPERLING

JOHNS HOPKINS UNIVERSITY
APPLIED PHYSICS LABORATORY
JOHNS HOPKINS ROAD
LAUREL, MD 20810
01CY ATTN DOCUMENT LIBRARIAN
01CY ATTN THOMAS POTEMRA
01CY ATTN JOHN DASSOULAS

KAMAN SCIENCES CORP
P.O. BOX 7463
COLORADO SPRINGS, CO 80933
01CY ATTN T. MEAGHER

KAMAN TEMPO-CENTER FOR ADVANCED STUDIES
816 STATE STREET (P.O DRAWER QQ)
SANTA BARBARA, CA 93102
01CY ATTN DASIAC
01CY ATTN WARREN S. KNAPP
01CY ATTN WILLIAM MCNAMARA
01CY ATTN B. GAMBILL

LINKABIT CORP
10453 ROSELLE
SAN DIEGO, CA 92121
01CY ATTN IRWIN JACOBS

LOCKHEED MISSILES & SPACE CO., INC
P.O. BOX 504
SUNNYVALE, CA 94088
01CY ATTN DEPT 60-12
01CY ATTN D.R. CHURCHILL

LOCKHEED MISSILES & SPACE CO., INC.
3251 HANOVER STREET
PALO ALTO, CA 94304
01CY ATTN MARTIN WALT DEPT 52-12
01CY ATTN W.L. IMHOF DEPT 52-12
01CY ATTN RICHARD G. JOHNSON, DEPT 52-12
01CY ATTN J.B. CLADIS DEPT 52-12

MARTIN MARIETTA CORP
ORLANDO DIVISION
P.O. BOX 5837
ORLANDO, FL 32805
01CY ATTN R. HEFFNER

M.I.T. LINCOLN LABORATORY
P.O. BOX 73
LEXINGTON, MA 02173
01CY ATTN DAVID M. TOWLE
01CY ATTN L. LOUGHLIN
01CY ATTN D. CLARK

MCDONNEL DOUGLAS CORPORATION
5301 BOLSA AVENUE
HUNTINGTON BEACH, CA 92647
01CY ATTN N. HARRIS
01CY ATTN J. MOULE
01CY ATTN GEORGE MROZ
01CY ATTN W. OLSON
01CY ATTN R.W. HALPRIN
01CY ATTN TECHNICAL LIBRARY SERVICES

MISSION RESEARCH CORPORATION
735 STATE STREET
SANTA BARBARA, CA 93101
01CY ATTN P. FISCHER
01CY ATTN W.F. CREVIER
01CY ATTN STEVEN L. GUTSCHE
01CY ATTN R. BOGUSCH
01CY ATTN R. HENDRICK
01CY ATTN RALPH KILB
01CY ATTN DAVE SOWLE
01CY ATTN F. FAJEN
01CY ATTN M. SCHEIBE
01CY ATTN CONRAD L. LONGMIRE
01CY ATTN B. WHITE
01CY ATTN R. STAGAT

MISSION RESEARCH CORP.
1720 RANDOLPH ROAD, S.E.
ALBUQUERQUE, NEW MEXICO 87106
01CY R. STELLINGWERF
01CY M. ALME
01CY L. WRIGHT

MITRE CORPORATION, THE
P.O. BOX 208
BEDFORD, MA 01730
01CY ATTN JOHN MORGANSTERN
01CY ATTN G. HARDING
01CY ATTN C.E. CALLAHAN

MITRE CORP
WESTGATE RESEARCH PARK
1820 DOLLY MADISON BLVD
MCLEAN, VA 22101
01CY ATTN W. HALL
01CY ATTN W. FOSTER

PACIFIC-SIERRA RESEARCH CORP
12340 SANTA MONICA BLVD.
LOS ANGELES, CA 90025
01CY ATTN E.C. FIELD, JR.

PENNSYLVANIA STATE UNIVERSITY
IONOSPHERE RESEARCH LAB
318 ELECTRICAL ENGINEERING EAST
UNIVERSITY PARK, PA 16802
(NO CLASS TO THIS ADDRESS)
01CY ATTN IONOSPHERIC RESEARCH LAB

PHOTOMETRICS, INC.
4 ARROW DRIVE
WOBURN, MA 01801
01CY ATTN IRVING L. KOFSKY

PHYSICAL DYNAMICS, INC.
P.O. BOX 3027
BELLEVUE, WA 98009
01CY ATTN E.J. FREMOUW

PHYSICAL DYNAMICS, INC.
P.O. BOX 10367
OAKLAND, CA 94610
ATTN A. THOMSON

R & D ASSOCIATES
P.O. BOX 9695
MARINA DEL REY, CA 90291
01CY ATTN FORREST GILMORE
01CY ATTN WILLIAM B. WRIGHT, JR.
01CY ATTN WILLIAM J. KARZAS
01CY ATTN H. ORY
01CY ATTN C. MACDONALD
01CY ATTN R. TURCO
01CY ATTN L. DeRAND
01CY ATTN W. TSAI

RAND CORPORATION, THE
1700 MAIN STREET
SANTA MONICA, CA 90406
01CY ATTN CULLEN CRAIN
01CY ATTN ED BEDROZIAN

RAYTHEON CO.
528 BOSTON POST ROAD
SUDBURY, MA 01776
01CY ATTN BARBARA ADAMS

RIVERSIDE RESEARCH INSTITUTE
330 WEST 42nd STREET
NEW YORK, NY 10036
01CY ATTN VINCE TRAPANI

SCIENCE APPLICATIONS, INC.
1150 PROSPECT PLAZA
LA JOLLA, CA 92037
01CY ATTN LEWIS M. LINSON
01CY ATTN DANIEL A. HAMLIN
01CY ATTN E. FRIEMAN
01CY ATTN E.A. STRAKER
01CY ATTN CURTIS A. SMITH

SCIENCE APPLICATIONS, INC
1710 GOODRIDGE DR.
MCLEAN, VA 22102
01CY J. COCKAYNE
01CY E. HYMAN

SRI INTERNATIONAL
333 RAVENSWOOD AVENUE
MENLO PARK, CA 94025
01CY ATTN J. CASPER
01CY ATTN DONALD NEILSON
01CY ATTN ALAN BURNS
01CY ATTN G. SMITH
01CY ATTN R. TSUNODA
01CY ATTN DAVID A. JOHNSON
01CY ATTN WALTER G. CHESNUT
01CY ATTN CHARLES L. RINO
01CY ATTN WALTER JAYE
01CY ATTN J. VICKREY
01CY ATTN RAY L. LEADABRAND
01CY ATTN G. CARPENTER
01CY ATTN G. PRICE
01CY ATTN R. LIVINGSTON
01CY ATTN V. GONZALES
01CY ATTN D. MCDANIEL

TECHNOLOGY INTERNATIONAL CORP
75 WIGGINS AVENUE
BEDFORD, MA 01730
01CY ATTN W.P. BOQUIST

TOYON RESEARCH CO.
P.O. Box 6890
SANTA BARBARA, CA 93111
01CY ATTN JOHN ISE, JR.
01CY ATTN JOEL GARBARINO

TRW DEFENSE & SPACE SYS GROUP
ONE SPACE PARK
REDONDO BEACH, CA 90278
01CY ATTN R. K. PLEBUCH
01CY ATTN S. ALTSCHULER
01CY ATTN D. DEE
01CY ATTN D/ STOCKWELL
SNTF/1575

VISIDYNE
SOUTH BEDFORD STREET
BURLINGTON, MASS 01803
01CY ATTN W. REIDY
01CY ATTN J. CARPENTER
01CY ATTN C. HUMPHREY

UNIVERSITY OF PITTSBURGH
PITTSBURGH, PA 15213
01CY ATTN: N. ZABUSKY

DIRECTOR OF RESEARCH
U.S. NAVAL ACADEMY
ANNAPOLIS, MD 21402 (02CY)

END

FILMED

6-85

DTIC